energies

MDPI

Article

Optimal Operation of Park and Ride EV Stations in Island Operation with Model Predictive Control

Soichiro Ueda [1,*], Atsushi Yona [1], Shriram Srinivasarangan Rangarajan [2,3], Edward Randolph Collins [3,4], Hiroshi Takahashi [5], Ashraf Mohamed Hemeida [6] and Tomonobu Senjyu [1]

1 Faculty of Engineering, University of the Ryukyus, Senbaru Nishihara-cho, Nakagami 903-0213, Japan
2 Department of Electrical and Electronics Engineering, Dayananda Sagar College of Engineering, Bengaluru 560078, India
3 Department of Electrical and Computer Engineering, Clemson University, Clemson, SC 29631, USA
4 College of Engineering, Western Carolina University, Cullowhee, NC 28723, USA
5 Fuji Electric Co., Ltd., Tokyo 141-0032, Japan
6 Department of Electrical Engineering, Aswan University, Aswan 82825, Egypt
* Correspondence: soichiro.55.ueda@gmail.com

Abstract: The urgent need to reduce greenhouse gas emissions to achieve a decarbonized society has led to the active introduction of electric vehicles worldwide. Renewable energy sources that do not emit greenhouse gases during charging must also be used. However, the uncertainty in the supply of renewable energy is an issue that needs to be considered in practical applications. Therefore, in this study, we predicted the amount of electricity generated by renewable energy using model predictive control, and we considered the operation of a complete island-operated park and ride EV parking station that does not depend on commercial electricity. To perform appropriate model predictive control, we performed comparative simulations for several different forecast interval cases. Based on the obtained results, we determined the forecast horizon and we simulated the economic impact of implementing EV demand response on the electricity demand side. We found that without demand response, large amounts of electricity are recharged and a very high return on investment can be achieved, but with demand response, the return on investment is faster. The results provide a rationale for encouraging infrastructure development in areas that have not yet adopted electric vehicles.

Keywords: electric vehicle; microgrid; model predictive control; park and ride; renewable energy

Citation: Ueda, S.; Yona, A.; Rangarajan, S.S.; Collins, E.R.; Takahashi, H.; Hemeida, A.M.; Senjyu, T. Optimal Operation of Park and Ride EV Stations in Island Operation with Model Predictive Control. *Energies* **2023**, *16*, 2468. https://doi.org/10.3390/en16052468

Academic Editors: Danial Karimi and Amin Hajizadeh

Received: 1 February 2023
Revised: 24 February 2023
Accepted: 3 March 2023
Published: 5 March 2023

1. Introduction

Efforts to reduce greenhouse gas emissions have recently gained momentum to achieve a carbon-neutral society. To reduce emissions by 46% by 2030 and achieve carbon neutrality by 2050, a strategy has been established in accordance with the Paris Agreement, and a policy to aggressively introduce electric vehicles (EVs) in the transportation sector strategy has been set [1]. However, if electricity derived from thermal power generation is used to charge EVs, greenhouse gases will be emitted in the process of charging EVs, and the benefits of EV deployment will be reduced. Therefore, we propose the use of renewable energy sources, such as photovoltaic (PV) and wind generation (WG), which do not emit greenhouse gases. We can choose to operate a facility in a microgrid using renewable energy, either grid-connected or independently operated. Both have advantages and disadvantages. Grid-connected operation allows for stable operation, but greenhouse gases are emitted due to the purchase of electricity that is not derived from renewable energy. With independent operation, the system is not connected to the existing grid, so the surrounding grid constraints do not need to be considered. In addition, because the system is assumed to be operated entirely with electricity derived from renewable energy, it can substantially contribute to the reduction in greenhouse gas emissions. However, facility

managers must solve the problem of unstable power sources with daily fluctuations in power generation. Several studies have been conducted on the combination of EVs and renewable energy [2–4]. We also propose that the above be implemented as a park and ride (P&R)-type EV parking station to reduce traffic congestion caused by private cars in urban areas and improve EV infrastructure.

Several researchers have discussed the problem of optimizing EV charging stations in a microgrid. Renewable energy sources such as PV and WG were introduced in one study, but the simulation period was one month, which is short [5]. The period was not continuous because specific days of the year were selected to compose a month. In another study [6], a simulation comparison was conducted on independently operated microgrids using the artificial bee colony (ABC) algorithm and the particle swarm optimization (PSO) algorithm, but the researchers focused on the comparison of methods and the simulation period was short (24 h), focusing on the operational waveforms. Researchers [7] considered an EV parking station connected to the grid (not an independent grid). PVs were installed as a power generation facility, but WG, which can generate power even at night, was not installed because power could be purchased from the grid at any time. In another study [8], PV and WG were considered for power generation facilities that could generate electricity 24 h per day. However, the researchers assumed a grid-connected microgrid, which limited the locations for building EV charging stations. The microgrid to which an EV charging parking station was connected was connected to the PV, WG, and storage batteries, and the structure was considered to be able to simultaneously meet the residential load [9]. This study also focused on a grid-connected system and described the phases of collecting EV charging information, controling the microgrid and allocating the generated electricity to the EVs. Grid connection provides considerable stability but at the cost of greenhouse gas emissions. In one study [10], Monte Carlo methods were used to generate random EV loads and describe operational optimization during recharging in the distribution network. However, the total computation time of the source code was 48 h, which is not computationally efficient. A one-year EV charging facility considering the island type has been proposed, and the impact of EV charging prices on EV charging profits has been discussed in [11]. To reduce CO_2 emissions, PVs can be used for power generation facilities. However, the available time for charging is limited because electricity cannot be generated at night. In addition, the service life of PVs has rarely been considered, so the long-term operation equivalent to the time of replacement of the power-generation equipment has not been taken into account. In another study [12], a distributed power control system that considers both grid-connected and independent operation was proposed. A system was constructed so that when the microgrid was separated from the grid supply for some reason, it became an independent operation. Independent operation causes problems such as power quality degradation, out of phase reclosure, loss of grounding, and safety concerns. The researchers proposed using a primary–secondary islanding scheme to survive the period of independent operation mode. In contrast, we built a model assuming an independent operation mode from the beginning, so the risk of the previously described problems [12] is very low.

As mentioned above, few examples exist of EV charging stations being considered as independent systems, and to the best of our knowledge, no study has yet addressed optimal scheduling for EV charging throughout the day and night during the year. Therefore, we considered the optimal operation of a stand-alone EV parking station where fine power regulation is possible. We assumed that each charging class in the station has its own guaranteed charging rate and that an operation schedule is constructed to meet this rate every day. In one aspect of balancing electricity supply and demand, vehicle-to-grid (V2G) can be applied in different ways. V2G is a method in which users of parking stations cooperate with each other by having EV owners sell electricity to parking station operators when electricity generation is low. Researchers [13,14] have described the operation of a power distribution network using V2G. One of the features of this method is that it allows power sales from EVs to help with charging other EVs and to allow appliances to operate.

However, the application of this method requires that there are many EV owners who are willing to sell electric power to the grid. In this study, EVs were assumed to be charged only, and a guarantee was provided regarding the EV charging rate. In principle, EVs are charged with electricity from renewable energy sources, and the guaranteed EV charging rate is relaxed when a shortage of electricity is forecasted. The two innovations of this study are as follows: The first is a simulation of the operation of a P&R-type EV charging station using model predictive control (MPC) and EV charge guarantee rate mitigation adjustment (demand response) for a full year. The second is the mitigation adjustment of the EV charging guarantee rate according to the amount of electricity generated in an independent EV charging parking station. The method of predicting electric power flow using MPC has often been employed [15,16]. This optimization problem can be expressed as a cost function minimization problem consisting of the initial and maintenance costs required to install power generation equipment, the charging revenues from selling electricity to EVs, and the EV parking fee revenues, which is transformed into a mixed integer linear programming (MILP) problem [17]. The contribution of this study is discovering the potential of island EV parking stations that do not rely on commercial electricity. By considering model predictive control and demand response in the system, we found that the instability of renewable energy can be substantially reduced and the return on investment can be increased.

The rest of this paper is organized as follows. Section 2 describes the proposed EV charging station model and the renewable energy to be installed. Section 3 describes the objective function and constraints of this study. Section 4 describes the simulation conditions and results. The different conditions for EVs are explained in this study. A comparative study of the two patterns is performed and the usefulness of the proposed method is discussed. Finally, Section 5 summarizes the results obtained, explains future steps, and concludes the paper.

2. EV Parking Station

In this study, the microgrid consists of photovoltaics (PVs), wind generation (WG), a battery energy storage system (BESS), and an electric vehicle (EV) charging station. The charging station is a park and ride (P&R) parking station, and the users have their own reasons for using the station, such as to reduce traffic congestion, reduce the burden on the environment, and move smoothly to their destinations. Figure 1 shows the model of the microgrid considered in this study. Electric power flows in the direction of the arrow. This microgrid was constructed for Urasoe, Okinawa Prefecture, Japan. In addition, the charging station has five classes with different charging priorities, one for daytime and one for nighttime; EV owners can select a class according to their own usage. These classes differ in recharge priority as well as recharge unit price, basic monthly fee, and recharge guarantee rate. In addition, a charge guarantee rate was set for each class to provide an appropriate guarantee for the class with the highest overall charge rate. Figure 2 shows the daily PV generation with a rated output of 500 kW by month from April 2019 to March 2020, and Figure 3 shows the daily generation of PV, with a rated output of 500 kW, by month. The electricity generated by the PV and WG is either used in charging the EV, stored in the BESS, or disposed of as surplus electricity.

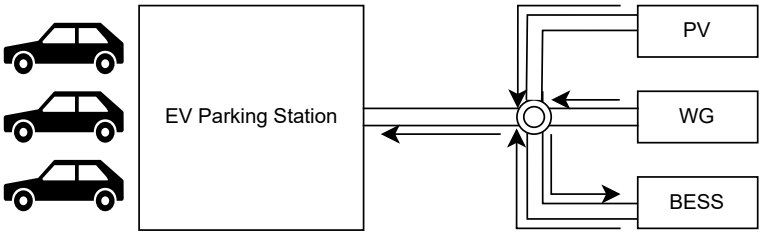

Figure 1. Microgrid model.

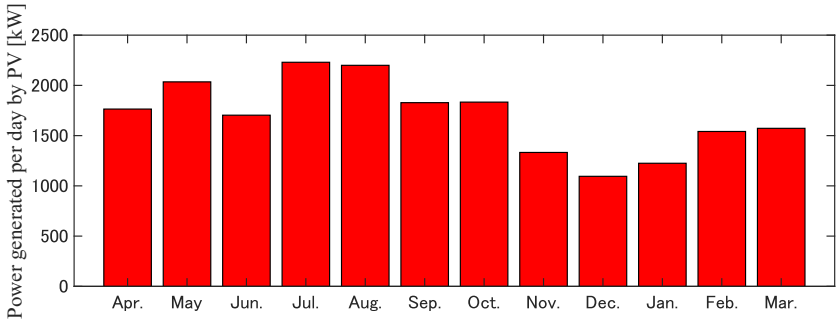

Figure 2. Daily generation of PV with a rated output of 500 kW by month.

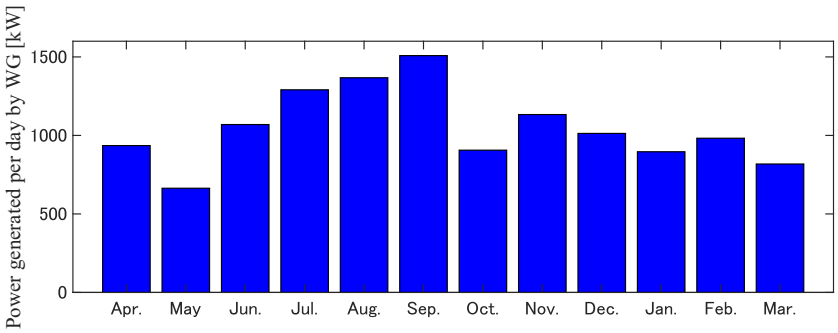

Figure 3. Daily generation of WG with a rated output of 250 kW by month.

In addition, model predictive control (MPC) is used to predict the amount of renewable energy generated up to a certain time. MPC is executed in the following steps.

(i) A control problem is solved based on an objective function and constraints over a predefined period of time to be controlled.
(ii) The first value of the obtained result is executed on the controlled object.
(iii) The time is advanced by one step and return to step (i).

This method allows for operational optimization at the present time considering the future several hours ahead. Notably, although predicting power generation farther into the future increases the stability of the system, it also increases the computational load.

3. Problem Formulation and Constraints

In this study, the optimization problem with the objective function and constraints formulated below is the operation of a P&R EV parking station for one year.

3.1. Objective Function

The objective function of the system includes PV, WG, and BESS facility costs and sale revenues to EV owners. To maximize the profit of the EV parking station operator, we determined the number of power generation facilities installed and the scheduling of BESS recharging and discharging.

$$min : C_{year} = C_{npv} + C_{nwg} + C_{nba} - \sum_{i}\sum_{t}\{R_{base}(i) \cdot 12 \cdot N_{EV}(i) + R_{ev}(i,t)\} \quad (1)$$

where C_{npv}, C_{nwg}, and C_{nba} are the annual PV, WG, and BESS equipment costs (JPY), respectively; $R_{base}(i)$ is the monthly basic charge for EV charging in class i (JPY); $N_{EV}(i)$ is the number of EVs in class i; R_{ev} is the revenue from electricity sales to EVs in class i at time t (JPY); and R_{ev} is the class i revenue from the sale of electricity to EVs at time t (JPY). C_{npv}, C_{nwg}, and C_{nba} are defined as follows:

$$C_{npv} = \frac{N_{pv} \cdot (I_{pv} + OM_{pv} \cdot LT_{pv})}{LT_{pv}} \quad (2)$$

$$C_{nwg} = \frac{N_{wg} \cdot (I_{wg} + OM_{wg} \cdot LT_{wg})}{LT_{wg}} \tag{3}$$

$$C_{nba} = \frac{N_{ba} \cdot I_{ba}}{LT_{ba}} \tag{4}$$

where N_{pv}, N_{wg}, and N_{ba} are the amounts of PV, WG, and BESS equipment, respectively; I_{pv}, I_{wg}, and I_{ba} are the initial costs of PV, WG, and BESS (JPY), respectively; OM_{pv} and OM_{wg} are the annual operational maintenance costs of PV and WG (JPY), respectively; and LT_{pv}, LT_{wg}, and LT_{ba} are the lifetimes of PV, WG, and BESS (years), respectively.

3.2. Constraints

To consider the EV charging and renewable energy optimization problem with a BESS, several constraints need to be satisfied.

To balance electricity supply and demand:

$$P_{PV,t} + P_{WG,t} + P_{BESSD,t} = P_{BESSC,t} + P_{EV,t} \tag{5}$$

where $P_{PV,t}$ and $P_{WG,t}$ are the amount of electricity generated by PV and WG at time t (kWh), respectively; $P_{BESSD,t}$is the amount of BESS discharged at time t (kWh); $P_{BESSC,t}$ is the amount of BESS charged at time t (kWh); and $P_{EV,t}$ is the amount of EV charged at time t (kWh).

For EV charging guarantee constraints:

$$0 \leq P_{EVC} \leq -P_{EVCap} - P_{EVE} \quad (t_{sta} \leq t \leq t_{fin}) \tag{6}$$

where P_{EVC} is the EV charge (kWh); P_{EVCap} is the EV storage battery capacity (kWh); P_{EVE} is the initial EV charge (kWh); t_{sta} is the EV arrival time; and t_{fin} is the EV departure time.

For EV charge rate constraints,

$$SOC_{minEV} \leq SOC_{EV,t} \leq SOC_{maxEV} \quad (t_i \leq t < t_o) \tag{7}$$

$$SOC_{gEV} \leq SOC_{EV,t} \leq SOC_{maxEV} \quad (t_o \leq t) \tag{8}$$

where SOC_{minEV} and SOC_{maxEV} are the minimum and maximum EV charging rates, respectively; $SOC_{EV,t}$ is the EV charging rate at time t; and SOC_{gEV} is the guaranteed EV charging rate.

For the BESS charge rate constraint:

$$20 \leq SOC_{BESS,t} \leq 100 \quad (\%) \tag{9}$$

where $SOC_{BESS,t}$ is the rate of charge of the BESS for any time t in the simulation period.

3.3. Model Predictive Control

The prediction period operation of the MPC algorithm is described by the following equation:

$$min : -\sum_{i} \sum_{t}^{t_{pred}} \{R_{base}(i) \cdot 12 \cdot N_{EV}(i) + R_{ev}(i,t)\} \tag{10}$$

where t_{pred} is the MPC forecast period. After calculating the optimal solution for this period, only the solution for the first step is saved. Next, the forecast period is shifted one step into the future. In this paper, one step is 24 h. The optimal solution for each period is saved and the calculation is repeated until all simulation optimal solutions are saved.

4. Simulation

In this section, we define several parameters that must be determined for the simulation and describe the results calculated based on these conditions.

4.1. Simulation Condition

Mixed integer linear programming (MILP), provided by MATLAB, was used to determine the optimal scheduling. The simulation period was 366 days from April 2019 to March 2020. We obtained the meteorological data for this period from the Japan Meteorological Agency website [18]. The sources of power to the microgrid for the P&R EV parking station include PV and WG, with an additional lithium-ion storage battery. The rated output and storage battery specifications for each installation are shown in Table 1. For the simulation, we used the prediction error, as shown in Figure 4. The prediction error is 0% at the current time (0 h), proportionally increases to 50% after 24 h, and is assumed to be constant at 50% after 24 h. The error is generated to the extent that it does not exceed the prediction error line shown in Figure 4 and affects the prediction of renewable energy generation. Figures 5–12 show the actual amount of electricity generated by the PV and WG1 units in April, July, October, and January, as well as the amount of electricity predicted by MPC.

Table 1. Specifications of each power generation facility and storage battery.

Parameter	Value
PV rated output	0.5 MW
WG rated output	0.25 MW
BESS performance	0.2 MW/1.2 MWh
BESS charge/discharge efficiency	90%
Initial charge rate of BESS	50%
Lifetime of PV	17 years
Lifetime of WG	17 years
Lifetime of BESS	6 years

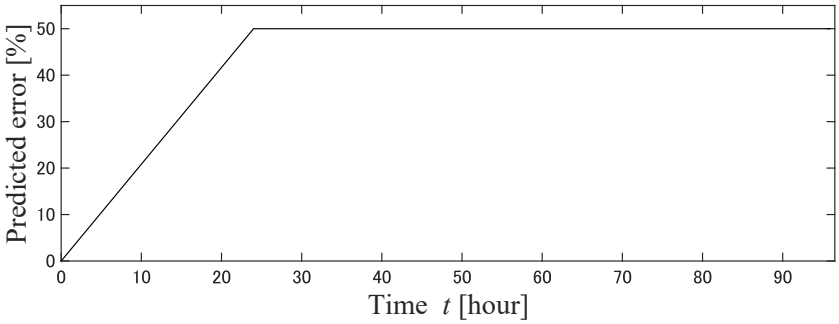

Figure 4. Upper limit of prediction error.

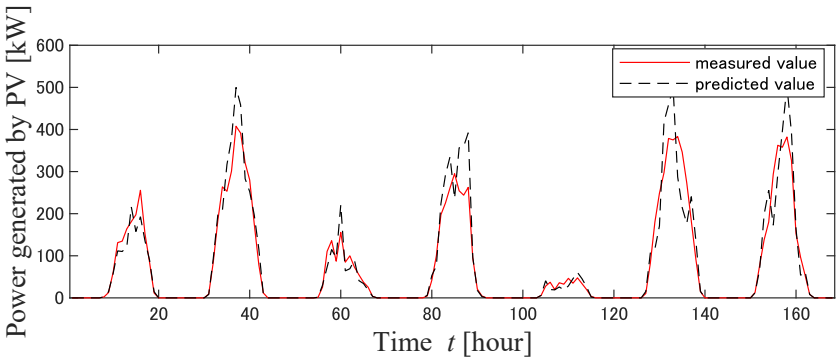

Figure 5. Generated power of PV (spring).

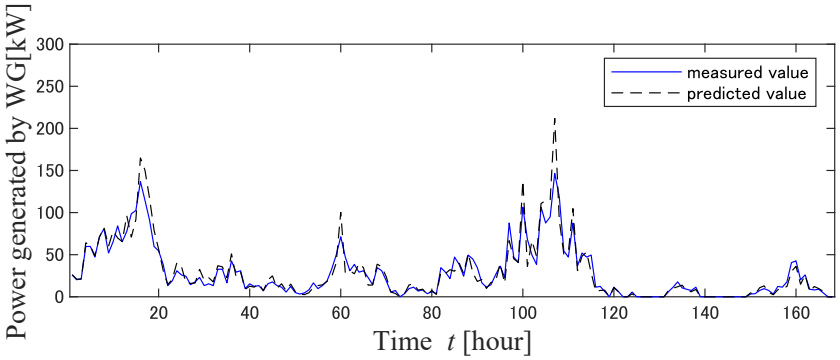

Figure 6. Power generated by WG (spring).

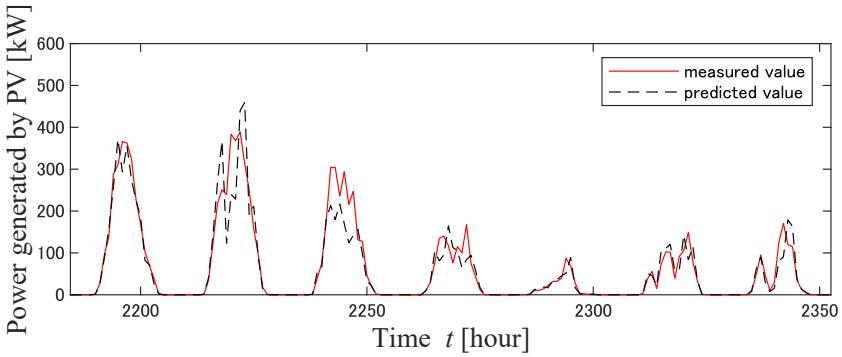

Figure 7. Power generated by PVs (summer).

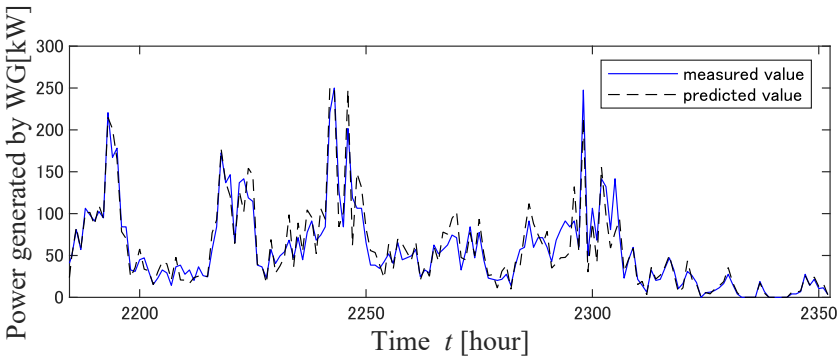

Figure 8. Power generated by WG (summer).

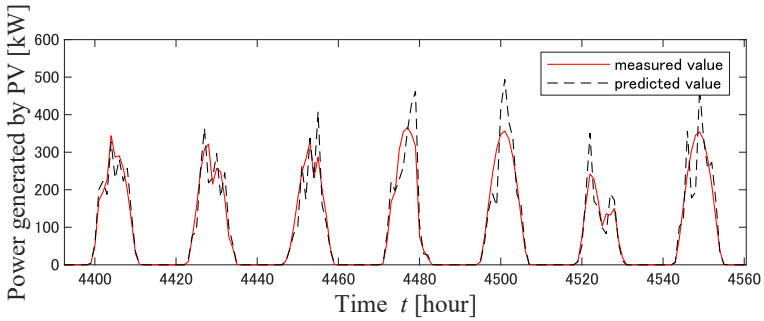

Figure 9. Power generated by PVs (autumn).

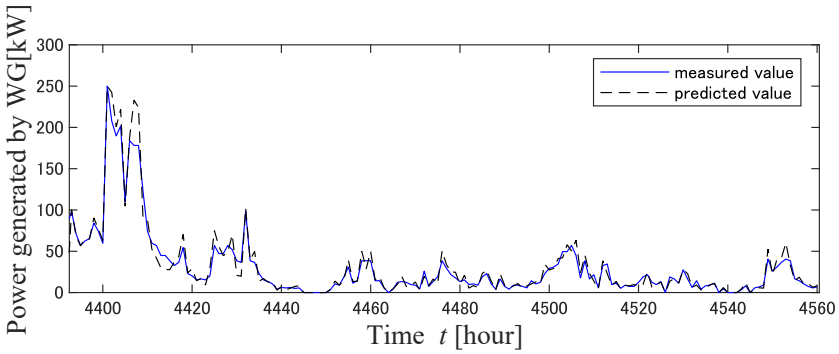

Figure 10. Power generated by WG (autumn).

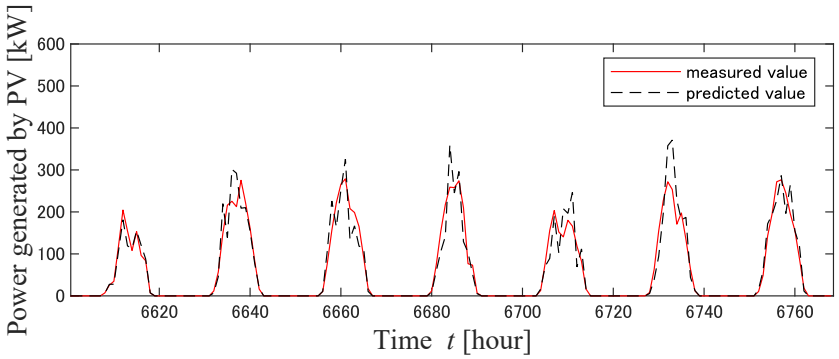

Figure 11. Power generated by PVs (winter).

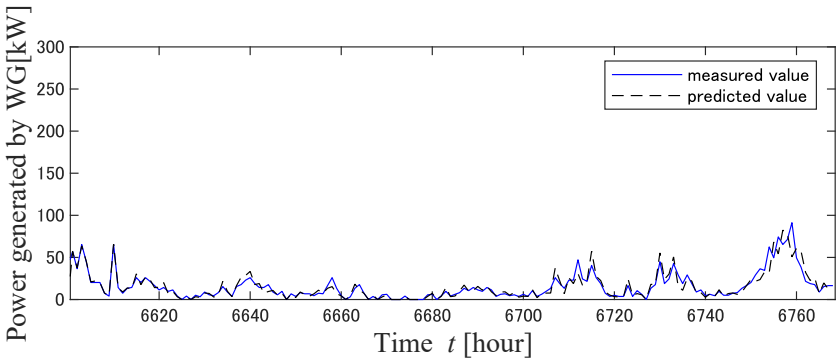

Figure 12. Power generated by WG (winter).

The generation waveforms show that the difference between the predicted and measured values increases over time. The number of EVs in the parking station was assumed to be 1000 during the day and 500 at night. In other words, the total number of active EVs is 1500 units. All EVs were assumed to have a storage battery capacity of 40 kWh and a charging efficiency of 0.9. The initial SOC of EVs coming to the parking station was assumed to be between 30% and 70%. The initial SOC of each EV was determined by a normal random number centered at 50%. We considered five day/night classes of EV parking stations, with a total of 10 classes, and each rate type is shown in Table 2. As a first comparative study to confirm the usefulness of MPC, the benefits of changing the forecast time to 24, 48, 72, and 96 h were considered. The number of EVs per class was assumed to be 5 classes with 200 EVs per class for daytime and 5 classes with 100 EVs per class for night-time.

Table 2. EV contract class.

Class Name	Power Rate (JPY/kWh)	Basic Rate (JPY/Month)
EV_1	35	12,000
EV_2	30	10,000
EV_3	25	9000
EV_4	20	8000
EV_5	15	7000
EV_{n1}	25	7000
EV_{n2}	20	6500
EV_{n3}	15	6000
EV_{n4}	10	5500
EV_{n5}	5	5000

For the second comparative study, the range to be projected by the MPC based on the considerations from the previous comparative study is determined. For EV charging stations, a minimum guaranteed charge rate was set for each class to differentiate the service between classes with higher and lower total charge rates. However, if there is insufficient power generation due to bad weather, it will be difficult to meet this guaranteed rate, which may lead to an unnecessary increase in the number of installations. Therefore, we will examine the impact on asset management by comparing the case where the guaranteed charge rate is changed according to the amount of electricity generated with the case where it is not changed. The number of EVs in each charging class assumed in this study is shown in Table 3. Table 4 shows the guaranteed rate for each EV class after mitigation adjustments and the guaranteed mitigation coverage. The mitigation tiers are expressed as levels, with lower and high daily generation resulting in higher and lower mitigation levels, respectively. Daily generation means the amount of electricity generated per day for the forecast period. The initial SOC of EVs arriving at the parking station is in a normal distribution with 50% as the average; therefore, the EVs may not charge at all if power generation is extremely low. As a result, the possibility of an imbalance between electricity supply and demand may be substantially reduced even on days when electricity generation is low. If the guaranteed rate is not changed, the mitigation level is assumed to be constant at 1.

Table 3. Number of EVs in each charging class (when mitigation conditions were changed).

Class Name	Number of EVs (Unit)
EV_1	360
EV_2	280
EV_3	120
EV_4	80
EV_5	160
EV_{n1}	100
EV_{n2}	100
EV_{n3}	100
EV_{n4}	100
EV_{n5}	100

Table 4. EV guaranteed mitigation levels and guaranteed mitigation coverage.

Level	EV_1	EV_2	EV_3	EV_4	EV_5	Daily Generation (kWh)
1	100	60	50	40	30	9000∼
2	80	60	50	40	30	8400∼9000
3	60	50	50	40	30	7200∼8400
4	60	50	40	30	30	6000∼7200
5	50	40	40	30	30	4500∼6000
6	40	40	30	30	30	∼4500

4.2. Simulation Results and Discussion

First, we conducted a comparative study of simulations with different forecasting periods to confirm the usefulness of MPC. The comparative study cases were as follows:

- Case 1: The MPC-predicted horizon is 24 h and the control horizon is 24 h.
- Case 2: The MPC-predicted horizon is 48 h and the control horizon is 24 h.
- Case 3: The MPC-predicted horizon is 72 h and the control horizon is 24 h.
- Case 4: The MPC-predicted horizon is 96 h and the control horizon is 24 h.

We do not discuss EV charging rates or detailed operational results here, as we focused on the benefits of the change in MPC forecast horizon. The results obtained from the comparison are shown in Table 5. The table shows the optimal number of units, annual profit, annual revenue, annual costs and their breakdown, and surplus power. The computation time for the one-year simulation was 62 s for Case 1, 137 s for Case 2, 182 s for Case 3, and 253 s for Case 4. Table 6 shows the internal rate of return (IRR) for these cases.

Table 5. Simulation results (when predicted horizon is changed).

Case	Number of PVs	Number of Wind Generators	Number of BESSs	Annual Profit (Million JPY)	Annual Revenue (Million JPY)	Annual Cost (Million JPY)	PV Cost (Million JPY)	WG Cost (Million JPY)	BESS Cost (Million JPY)	Surplus (MWh)
1 (24 h)	5	2	14	83	239	157	45	20	92	26.6
2 (48 h)	6	1	10	118	247	129	53	10	66	91.8
3 (72 h)	6	2	7	144	264	120	53	20	46	165.6
4 (96 h)	5	2	8	143	260	117	45	20	52	31.2

Table 6. IRR and cumulative profit (when predicted horizon is changed) *1.

	Case 1		Case 2		Case 3		Case 4	
Year	IRR	Cumulative Profit (Million JPY)	IRR	Cumulative Profit (Million JPY)	IRR	Cumulative Profit (Million JPY)	IRR	Cumulative Profit (Million JPY)
	(Initial investment)	−1312	(Initial investment)	−1174	(Initial investment)	−1151	(Initial investment)	−1076
1	−85.57%	−1123	−83.00%	−974	−81.63%	−940	−80.49%	−866
2	−54.13%	−934	−49.40%	−775	−46.98%	−728	−45.00%	−656
3	−32.52%	−744	−27.36%	−575	−24.76%	−517	−22.65%	−446
4	−18.87%	−555	−13.82%	−375	−11.27%	−305	−9.22%	−236
5	−9.99%	−366	−5.18%	−176	−2.76%	−94	−0.82%	−26
6	−3.98%	−176	0.57%	24	2.86%	118	4.70%	184
7	(*2)	−538	−5.37%	−170	1.40%	54	2.27%	79
8	−9.17%	−348	0.68%	29	5.49%	266	6.50%	289
9	−3.06%	−159	4.24%	229	8.21%	477	9.27%	499
10	0.47%	30	6.66%	429	10.15%	689	11.21%	709

*1 Add JPY 30 million per year in labor as the cost. *2 IRR calculation was not possible because of the rapid decline in profits due to equipment replacement.

By examining the IRR for each year, we could compare the rate of return, which could not be read from just one year's income and expenses. In this study, we calculated IRRs up to 10 years into the future. In addition to capital investment, labor costs were considered when calculating the IRR. In this case, we assumed that JPY 30 million is allocated to labor costs each year. From the results in Table 5, we confirmed that the annual profit increases from 24 to 72 h in advance, but from 72 to 96 h in advance, the annual profit does not increase; on the contrary, it decreases. Here, we focused on the IRR for the next 10 years to obtain information that cannot be read only from the change in annual profit. After the initial investment is completed, OM costs and labor costs are required each year for each facility. At the end of the useful life of the equipment, additional initial costs for a number of units are incurred for replacement. The IRR for the 24- and 48-h-ahead cases were markedly lower than for the other two situations. Both the 72- and 96-h-ahead cases

are expected to be profitable after the sixth year, but the 96-h-ahead case has a higher return. Based on the above results, in the next comparative study, we simulated the MPC with the 96-h-ahead forecast, which has a higher return.

Next, we discussed the simulation results related to the mitigation adjustment of the guaranteed charge rate. Based on the results of the first comparison study, we used MPC with a forecast horizon of 96 h and a control horizon of 24 h. The comparative cases were as follows:

- Case 1: No mitigation adjustment.
- Case 2: With six levels of mitigation adjustment.

The obtained optimal number of units, annual profit, annual revenue, annual cost and its breakdown, and excess power are shown in Table 7. The computation time for the one-year simulation was 119 s for Case 1 and 111 s for Case 2. Figures 13–16 show the generation and consumption of Case 1 in spring, summer, fall, and winter and Figures 17–20 show the recharge rate of the BESS. Similarly, Figures 21–24 show the generation and consumption for Case 2 and Figures 25–28 show the BESS charge rate. The EV charging rates for each class are shown in Table 8. Table 9 shows the IRR considering an annual labor cost of JPY 30 million. Table 7 shows that the profit without mitigation adjustment is higher than that with mitigation adjustment. Table 8 confirms that the reason for this is that the amount of electricity used to charge the EVs is also higher because no mitigation adjustment is applied. However, this is achieved at the cost of requiring more power generation equipment and storage batteries, i.e., higher annual costs. We focus on the IRR in Table 9. In the case with mitigation adjustment, the investment payback is achieved in the sixth year, whereas in the case without mitigation adjustment, the investment payback is not achieved even by the tenth year. This indicates that it is better to include charging mitigation adjustments in the operation of park and ride EV charging facilities. Note Figures 14, 18, 22 and 26. These figures show that power generation declined after July 4.

For MPC, which forecasts 96 h ahead, this phenomenon could be predicted as early as July 1. During this period, the SOC of the BESS is trying to keep the battery as fully charged as possible to cope with the periods when power generation is scarce. This allows the BESS to operate from July 4 to 7 while discharging the power stored in the BESS.

Table 7. Simulation results (when the mitigation conditions were changed).

Case	Number of PVs	Number of Wind Genera-tors	Number of BESSs	Annual Profit (Million JPY)	Annual Revenue (Million JPY)	Annual Cost (Million JPY)	PV Cost (Million JPY)	WG Cost (Million JPY)	BESS Cost (Million JPY)	Surplus (MWh)
1 (no mitigation)	14	6	13	127	398	271	125	61	85	1202
2 (with mitigation)	6	2	6	158	272	113	53	20	39	195

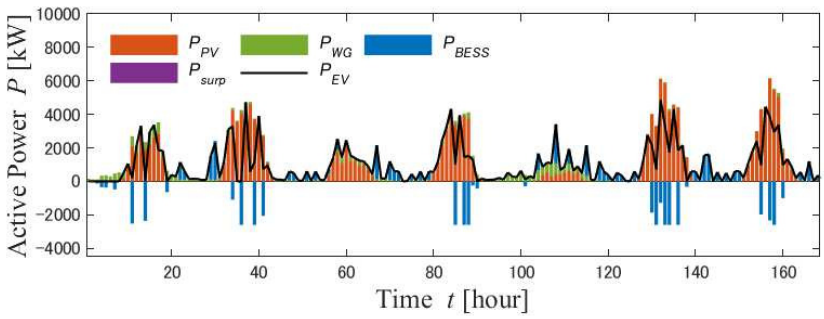

Figure 13. Generated power and load from April 1 to 7 (Case 1).

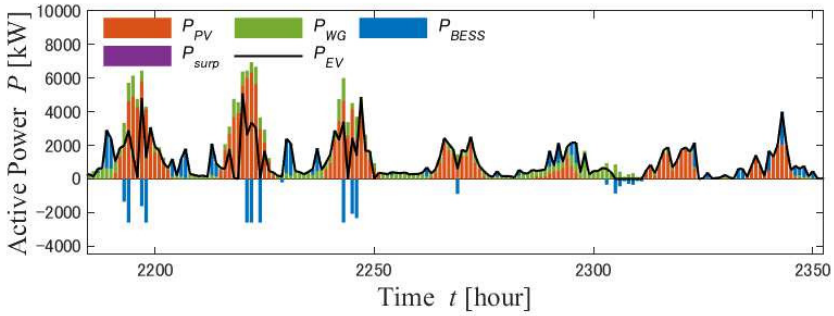

Figure 14. Generated power and load from July 1 to 7 (Case 1).

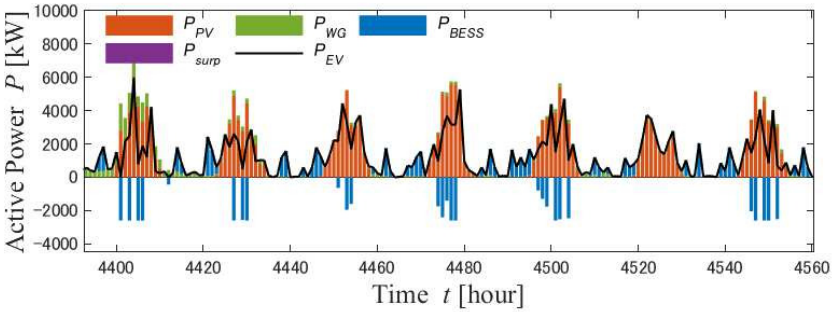

Figure 15. Generated power and load from October 1 to 7 (Case 1).

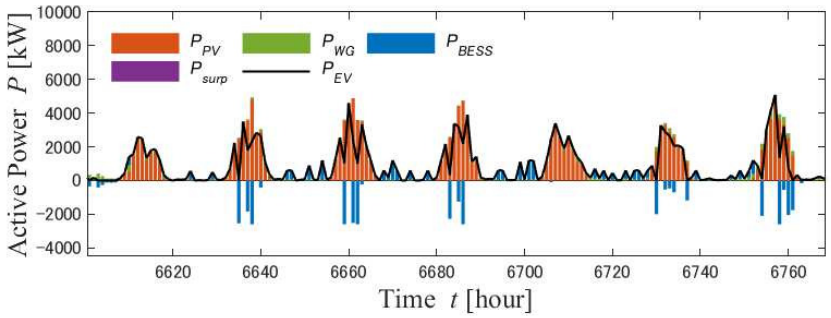

Figure 16. Generated power and load from January 1 to 7 (Case 1).

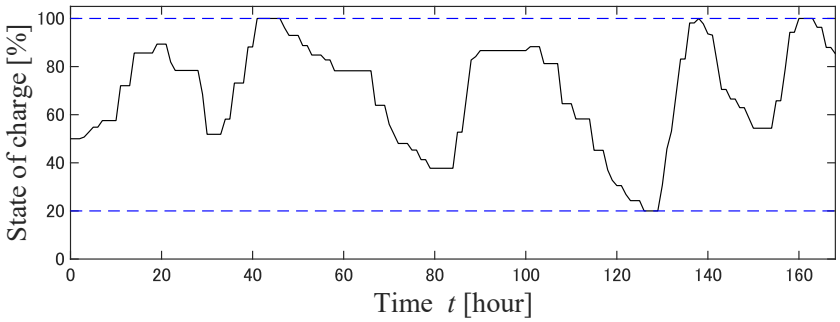

Figure 17. SOC of BESS from April 1 to 7 (Case 1).

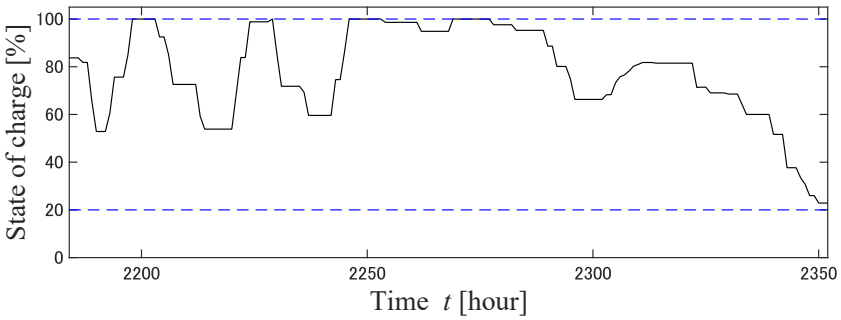

Figure 18. SOC of BESS from July 1 to 7 (Case 1).

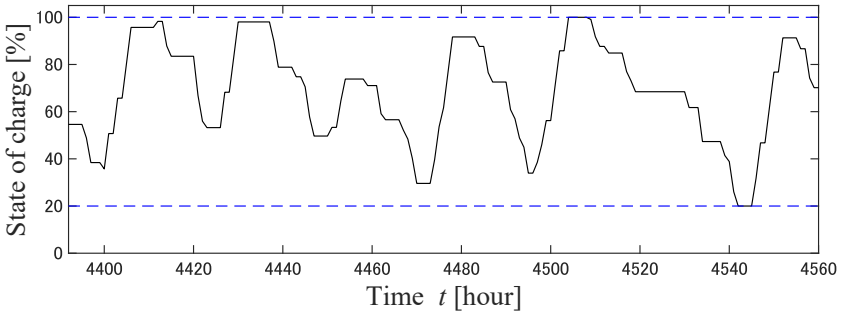

Figure 19. SOC of BESS from October 1 to 7 (Case 1).

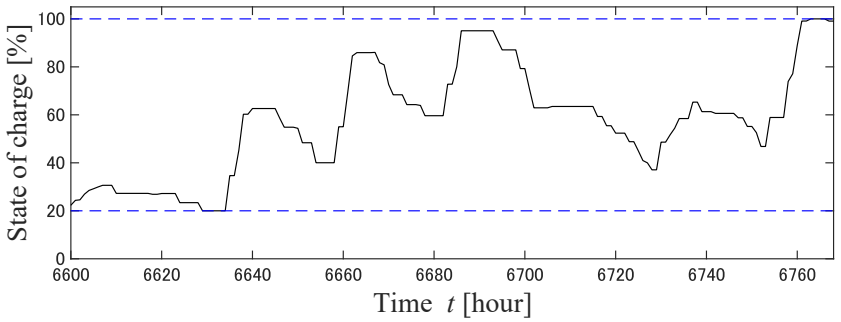

Figure 20. SOC of BESS from January 1 to 7 (Case 1).

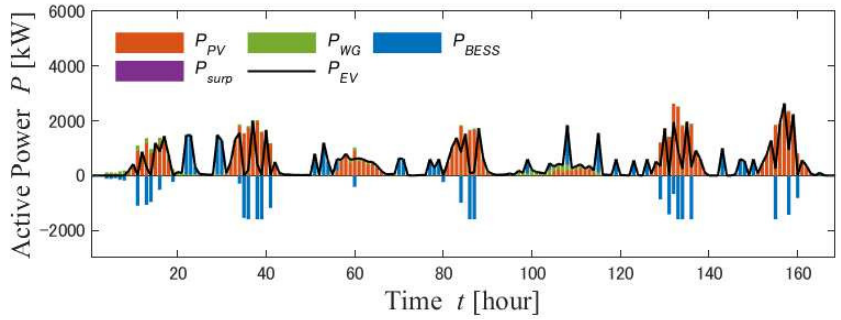

Figure 21. Generated power and load from April 1 to 7 (Case 2).

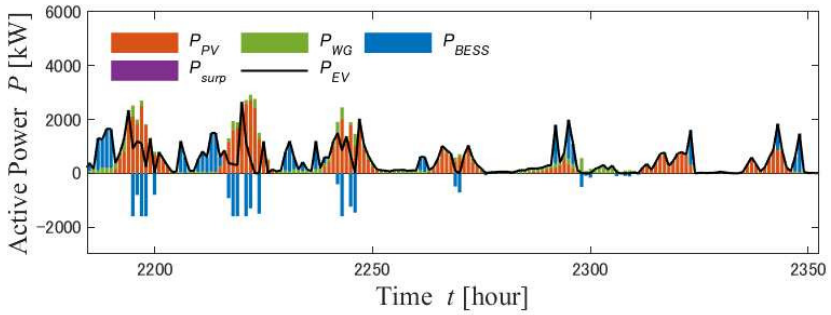

Figure 22. Generated power and load from July 1 to 7 (Case 2).

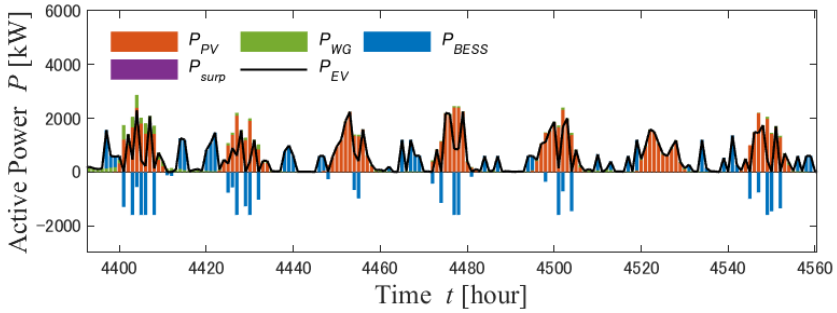

Figure 23. Generated power and load from October 1 to 7 (Case 2).

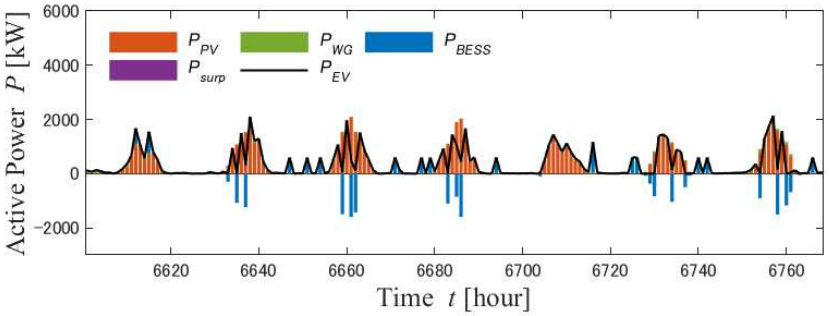

Figure 24. Generated power and load from January 1 to 7 (Case 2).

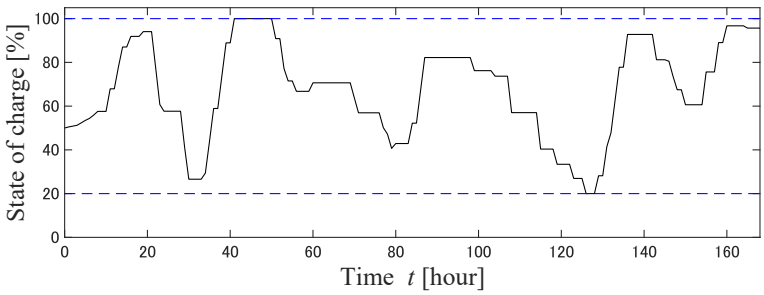

Figure 25. SOC of BESS from April 1 to 7 (Case 2).

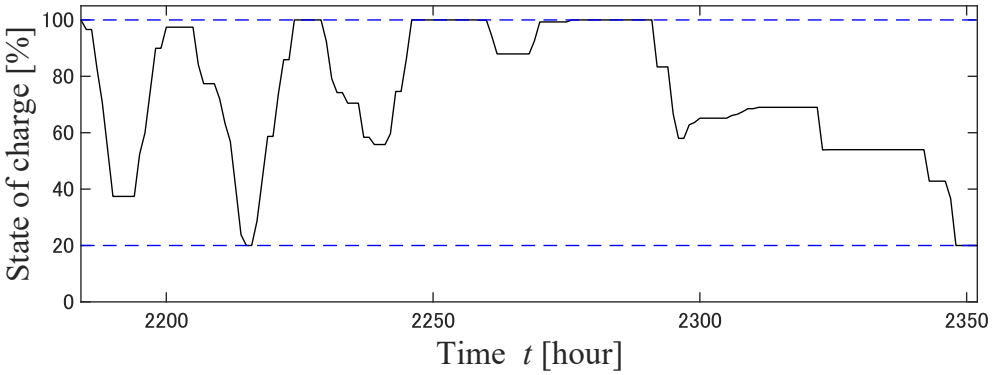

Figure 26. SOC of BESS from July 1 to 7 (Case 2).

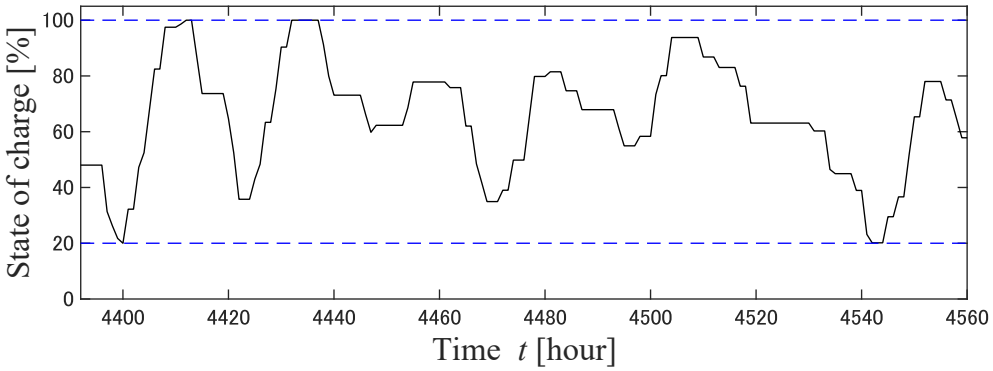

Figure 27. SOC of BESS from October 1 to 7 (Case 2).

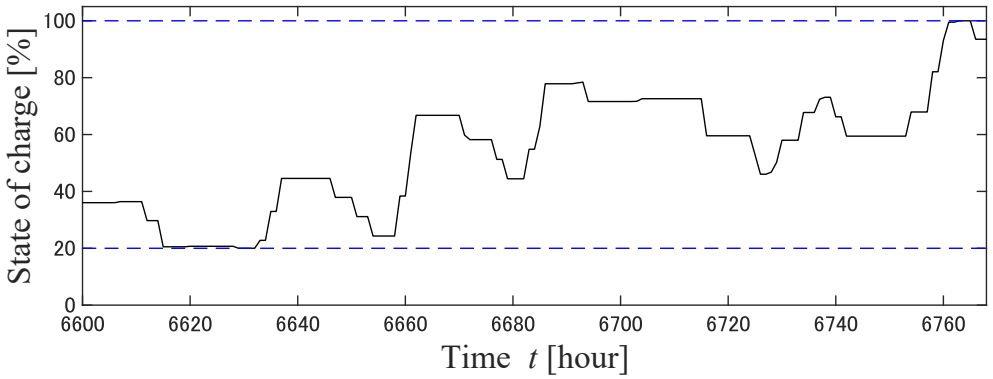

Figure 28. SOC of BESS from January 1 to 7 (Case 2).

Table 8. EV charging rates (when mitigation conditions are changed).

Case	EV_1 (%)	EV_2 (%)	EV_3 (%)	EV_4 (%)	EV_5 (%)	EV_{n1} (%)	EV_2 (%)	EV_3 (%)	EV_4 (%)	EV_5 (%)
1 (no mitigation)	100	99.7	98.8	95.2	85.9	98.9	93.6	82.7	73.4	67.6
2 (with mitigation)	79.9	68.8	66.7	57.0	54.0	91.5	74.1	61.2	54.0	50.1

Table 9. IRR and cumulative profit (when mitigation conditions are changed) *3.

Year	Case 1		Case 2	
	IRR	**Cumulative Profit (Million JPY)**	**IRR**	**Cumulative Profit (Million JPY)**
	(Initial investment)	−2682	(Initial investment)	−1112
1	−88.43%	−2372	−80.27%	−893
2	−59.72%	−2061	−44.64%	−673
3	−38.73%	−1752	−22.26%	−454
4	−25.01%	−1441	−8.85%	−235
5	−15.86%	−1131	−0.46%	−15
6	−9.53%	−821	5.04%	204
7	−13.98	−1022	4.70%	188
8	−7.36%	−711	8.28%	407
9	−3.40%	−401	10.73%	626
10	−0.66%	91	12.48%	846

*3 Add JPY 30 million per year in labor costs.

5. Conclusions

In this study, we investigated the optimal design of a park and ride EV charging station with PV, wind, and Li-ion batteries. The objective function consisted of PV, WP, and BESS facility costs and sales revenue to EV owners, which we set to maximize annual profit. In this study, model predictive control was used, and a comparative study with different forecast horizons was conducted to find the optimal conditions for model predictive control. The results showed that the longer the forecast horizon, i.e., the farther into the future was forecast, the higher the annual profit or IRR. Extending the forecast horizon allows more flexibility in the operation of stationary storage batteries. Based on the obtained results, a comparative study was conducted using model predictive control that predicted 96 h in advance, with and without mitigation adjustment to the guaranteed charge rate. The results showed that without the mitigation adjustment, the annual EV charge rate was higher, but so was the facility cost. With mitigation adjustment, the annual revenue of EVs was slightly lower, but equipment costs were lower and annual profits were higher. Furthermore, by focusing on IRR, we found that a faster return on investment could be achieved in cases where mitigation adjustments are applied.

If the number of park and ride EV stations increases, EV users will be able to choose either a plan with a high charging rate or the station itself at the expense of cost. However, not many EV parking stations currently exist in Japan. The infrastructure for EVs should be established as soon as possible by adopting a plan that provides a good return on investment.

Author Contributions: Conceptualization, S.U., A.Y., S.S.R., E.R.C., H.T., A.M.H. and T.S.; methodology, S.U. and T.S.; software, S.U.; validation, S.U.; investigation, T.S.; resources, S.U.; data curation, S.U.; Writing – original draft, S.U.; Visualization, S.U.; Supervision, T.S. All authors have read and agreed to the published version of the manuscript.

Funding: This study received no external funding.

Data Availability Statement: Data sharing is not applicable to this article.

Conflicts of Interest: The authors declare no conflicts of interest.

References

1. Ministry of the Environment (MOE), Consideration for 2030. Available online: https://www.enecho.meti.go.jp (accessed on 7 January 2023).
2. Strunz, K.; Abbasi, E.; Huu, D.N. DC Microgrid for Wind and Solar Power Integration. *IEEE J. Emerg. Sel. Top. Power Electron.* **2014**, *2*, 115–126. [CrossRef]
3. Liu, C.; Chau, K.T.; Wu, D.; Gao, S. Opportunities and Challenges of Vehicle-to-Home, Vehicle-to-Vehicle, and Vehicle-to-Grid Technologies. *Proc. IEEE* **2013**, *101*, 2409–2427. [CrossRef]

4. Zhang, T.; Chen, W.; Han, Z.; Cao, Z. Charging Scheduling of Electric Vehicles with Local Renewable Energy Under Uncertain Electric Vehicle Arrival and Grid Power Price. *IEEE Trans. Veh. Technol.* **2014**, *63*, 2600–2612. [CrossRef]
5. Takahashi, K.; Masrur, H.; Nakadomari, A.; Narayanan, K.; Takahashi, H.; Senjyu, T. Optimal Sizing of a Microgrid System with EV Charging Station in Park & Ride Facility. In Proceedings of the 12th IEEE PES Asia-Pacific Power and Energy Engineering Conference (APPEEC), Nanjing, China, 20–23 September 2020; pp. 1–4. [CrossRef]
6. Habib, H.U.; Waqar, A.; Hussien, M.G.; Junejo, A.K.; Jahangiri, M.; Imran, R.M.; Kim, Y.S.; Kim, J.H. Analysis of Microgrid's Operation Integrated to Renewable Energy and Electric Vehicles in View of Multiple Demand Response Programs. *IEEE Access* **2022**, *10*, 7598–7638. [CrossRef]
7. Çiçek, A.; Şengör, İ.; Güner, S.; Karakuş, F.; Erenoğlu, A.K.; Erdinç, O.; Shafie-Khah, M.; Catalão, J.P. Integrated Rail System and EV Parking Lot Operation With Regenerative Braking Energy, Energy Storage System and PV Availability. *IEEE Trans. Smart Grid* **2022**, *13*, 3049–3058. [CrossRef]
8. Zhang, M.; Chen, J. The Energy Management and Optimized Operation of Electric Vehicles Based on Microgrid. *IEEE Trans. Power Deliv.* **2014**, *29*, 1427–1435. [CrossRef]
9. Jiao, F.; Zou, Y.; Zhang, X.; Zhang, B. A Three-Stage Multitimescale Framework for Online Dispatch in a Microgrid With EVs and Renewable Energy. *IEEE Trans. Transp. Electrif.* **2022**, *8*, 442–454. [CrossRef]
10. Lazarou, S.; Vita, V.; Christodoulou, C.; Ekonomou, L. Calculating Operational Patterns for Electric Vehicle Charging on a Real Distribution Network Based on Renewables' Production. *Energies* **2018**, *11*, 2400. [CrossRef]
11. Shaaban, M.F.; Mohamed, S.; Ismail, M.; Qaraqe, K.A.; Serpedin, E. Joint Planning of Smart EV Charging Stations and DGs in Eco-Friendly Remote Hybrid Microgrids. *IEEE Trans. Smart Grid* **2019**, *10*, 5819–5830. [CrossRef]
12. Ekonomou, L.; Fotis, G.P.; Vita, V.; Mladenov, V. Distributed generation islanding effect on distribution networks and end user loads using the master-slave islanding method. *J. Power Energy Eng.* **2016**, *4*, 1–24. [CrossRef]
13. Li, S.; Zhao, P.; Gu, C.; Li, J.; Cheng, S.; Xu, M. Battery Protective Electric Vehicle Charging Management in Renewable Energy System. *IEEE Trans. Ind. Inform.* **2023**, *19*, 1312–1321. [CrossRef]
14. Vita, V.; Koumides, P. Electric Vehicles and Distribution Networks: Analysis on Vehicle to Grid and Renewable Energy Sources Integration. In Proceedings of the 11th Electrical Engineering Faculty Conference (BulEF), Varna, Bulgaria, 11–14 September 2019; pp. 1–4. [CrossRef]
15. Wang, T.; O'Neill, D.; Kamath, H. Dynamic Control and Optimization of Distributed Energy Resources in a Microgrid. *IEEE Trans. Smart Grid* **2015**, *6*, 2884–2894. [CrossRef]
16. Guo, Y.; Xiong, J.; Xu, S.; Su, W. Two-Stage Economic Operation of Microgrid-Like Electric Vehicle Parking Deck. *IEEE Trans. Smart Grid* **2016**, *7*, 1703–1712. [CrossRef]
17. Mathworks. Mixed-Integer Linear Programming (MILP). Available online: https://www.mathworks.com/help/optim/ug/intlinprog.html (accessed on 12 January 2023).
18. Japan Meteorological Agency (JMA). Historical Weather Data Search. Available online: http://www.data.jma.go.jp/ (accessed on 7 January 2023).